Looking for an Invisible Higgs Signal at the LHC

Diptimoy Ghosh [a,1], Rohini Godbole [b,2], Monoranjan Guchait [c,3] Kirtimaan Mohan [b,4] and Dipan Sengupta [c,5]

[a)] INFN, Sezione di Roma,
Piazzale A. Moro 2, I-00185 Roma, Italy.

[b)] Center for High Energy Physics, Indian Institute of Science,
Bangalore, 560012, India.

[c)] Department of High Energy Physics, Tata Institute of Fundamental Research,
1, Homi Bhabha Road, Mumbai 400 005, India.

Abstract

While the recent discovery of a Higgs-like boson at the LHC is an extremely important and encouraging step towards the discovery of the *complete* standard model(SM), the current information on this state does not rule out possibility of beyond standard model (BSM) physics. In fact the current data can still accommodate reasonable values of the branching fractions of the Higgs into a channel with 'invisible' decay products, such a channel being also well motivated theoretically. In this study we revisit the possibility of detecting the Higgs in this invisible channel for both choices of the LHC energies, 8 and 14 TeV, for two production channels; vector boson fusion(VBF) and associated production(ZH). In the latter case we consider decays of the Z boson into a pair of leptons as well as a $b\bar{b}$ pair. For the VBF channel the sensitivity is found to be more than 5σ at both the energies up to an invisible branching ratio $\mathcal{B}r_{invis} \sim 0.80$, with luminosities $\sim 20/30\text{fb}^{-1}$. The sensitivity is further extended to values of $\mathcal{B}r_{invis} \sim 0.25$ for 300 fb^{-1} at 14 TeV. However the reach is found to be more modest for the ZH mode with leptonic final state; with about 3.5σ for the planned luminosity at 8 TeV, reaching 8σ only for 14 TeV for 50 fb^{-1}. In spite of the much larger branching ratio of the Z into a $b\bar{b}$ channel compared to the dilepton case, the former channel, can provide useful reach upto $\mathcal{B}r_{invis} \gtrsim 0.75$, only for the higher luminosity (300 fb^{-1}) option using jet-substructure and jet clustering methods for b-jet identification.

[1]diptimoy.ghosh@roma1.infn.it [2]rohini@cts.iisc.ernet.in [3]guchait@tifr.res.in [4]kirtimaan@cts.iisc.ernet.in [5]dipan@tifr.res.in

1 Introduction

The unprecedented high precision to which the Standard Model (SM) [1, 2, 3] has been tested as well as the discovery of a Higgs like boson at both the ATLAS and CMS [4, 5] notwithstanding, the deficiencies of the Standard model (SM) both of the observational [6, 7] and aesthetic nature are substantial to justify the existence of physics beyond the Standard Model (BSM). For example, the instability of the electroweak scale under radiative corrections is cured by several BSM models. So far the Large Hadron Collider (LHC) has not given us any evidence of BSM physics. The recent discovery of a Higgs like boson at both the ATLAS and CMS [4, 5] experiments has opened up new avenues for discovering or restricting the possibility of various BSM scenarios. Since many of the extensions of the SM have been suggested to address the issue of stability of the electroweak symmetry breaking scale against radiative corrections, all of them have implications for properties of the Higgs sector such as the number of the Higgs bosons and their couplings and CP properties. Hence it is very likely that a study of the properties of this boson can also yield information about BSM physics. A clear understanding of the characteristics of the Higgs will elucidate not only the nature of electroweak symmetry breaking (EWSB), but also help in our understanding of how a BSM spectrum may generate or be part of EWSB. The lack of appearance at the LHC of any other particle, not expected in the SM, so far in fact means that the properties of the Higgs may therefore, give us our first glimpse at BSM physics.

Of course the first important step in establishing the new boson which we have discovered as 'a' Higgs boson, will be to have some pointers to the spin and CP of the state. However, finally, the identification of this boson as the particle responsible for EWSB requires the determination of its coupling to fermions and gauge bosons. Let us note that the tree level couplings of the Higgs to the fermions and the electroweak gauge bosons, are completely determined by the details of the EWSB. On the other hand the loop induced couplings of the Higgs to a pair of gg and $\gamma\gamma$, as well as the higher dimensional operators in other couplings can receive contributions from BSM physics as well. Hence, the measurement of the relative decay widths of the Higgs into different final states will not only provide information about the EWSB mechanism but may also carry with it information about BSM particle spectra. For example, the apparent excess of events seen in the $H \to \gamma\gamma$ channel coupled with non observation in the $H \to \tau\tau$ channel [4, 5], if confirmed, will have strong implications for various BSM models.

Strong cosmological evidence supporting the existence of Dark Matter (DM) means that almost all extensions of SM must include in their spectra a candidate for it which is supposed to be neutral and weakly interacting. A large number of such models allow for a significant branching fraction

for the decay of the Higgs to DM, thus providing a channel where the Higgs decay is "invisible" to the detector. In the SM the Higgs can decay invisibly through $H \to ZZ^* \to 4\nu$, which can only contribute to roughly 0.1% of the branching ratio [8]. Therefore, the observation of a sizable invisible branching ratio ($\mathcal{B}r_{invis}$) of the Higgs will be a strong indication for BSM physics. There exist several examples of BSM physics models where the Higgs can have an invisible decay, such as, the decay of the Higgs to the lightest supersymmetric particle (LSP) [9], decay to graviscalars in extra-dimensional models [10, 11] in gauge extensions of the SM [12] and in models for neutrino masses [13]. If the boson that has been observed at the LHC is the Higgs, then the currently available data can constrain the size of $\mathcal{B}r_{invis}$[14, 15]. Global fits to the LHC data suggest that an invisible branching ratio as large as 0.64 of the Higgs of mass ∼125 GeV is still allowed by the current data [14, 15, 16]. In fact detailed analysis of LEP data showed no evidence for an invisibly decaying of mass less than 112.1 GeV [17].

The feasibility of determining an invisible branching fraction of the Higgs at the LHC has been studied in various production modes of the Higgs [18, 19, 20, 21, 22, 23, 24] which is described very briefly in the next section. We look at the production of Higgs in association with a electroweak gauge boson as well as through Vector Boson Fusion (VBF) in detail. In earlier studies, the leptonic decay of the Z boson was used to identify the invisible decay of a Higgs produced in association with a Z boson [21]. In the present study we update the analysis in the leptonic channel and also probe the possibility of detecting an invisible decay of the Higgs by identifying the associated Z boson through b-tagged jets both for 8 TeV and as well as 14 TeV LHC. We also apply the jet-substructure algorithm [25] for b-tagged final states which marginally help in improving signal acceptance efficiencies. In addition, we study how the invisible decay channel can be probed in the production of the Higgs via vector boson fusion for both 8 TeV and 14 TeV LHC energy.

We organize our work as follows. In section 2, we discuss very briefly about the invisible decay of Higgs. In the subsequent sections 3 and 4, we describe simulation of invisible Higgs signal for VBF and ZH channels. Finally, we summarize our observations in section 5.

2 Signatures of an invisibly decaying Higgs

There are four main production mechanisms of the Higgs boson in a hadron collider. The most dominant one is gluon-gluon fusion via a top quark loop (ggF) ($gg \to H$) followed by VBF ($q\bar{q} \to q\bar{q}H$), Higgs production in association with vector bosons (VH) ($q\bar{q} \to ZH/WH$) and finally in association with top pairs (ttH) ($gg/q\bar{q} \to t\bar{t}H$) with the lowest cross section [26, 27, 28, 29, 30, 31, 32]. The various production channels are shown in Fig. 1. Needless to say that the signature of the

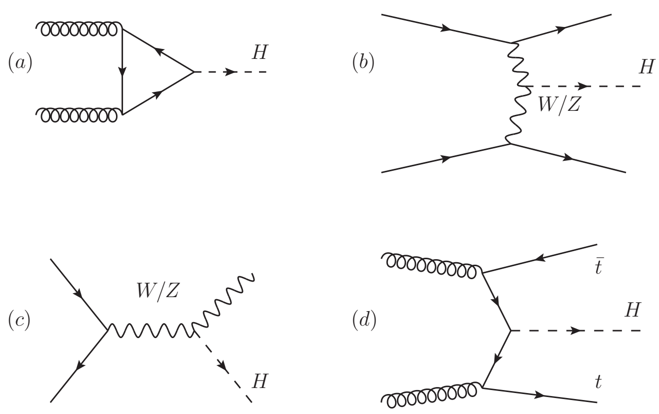

Figure 1: Higgs production channels at the LHC: (a)gluon-gluon fusion(ggF), (b) Vector boson fusion(VBF), associated productions (c) ZH and (d) $t\bar{t}H$

.

Higgs particle are characterized by the pattern of the Higgs decay channels [33]. Recall that the BR of the Higgs decay in the invisible channel in the framework of SM is too low to observe, therefore, any observation of invisible decay channel of the Higgs will shed some light about BSM physics. On the other hand the production cross section of the Higgs can vary in various models due to the presence of new particles inside loops and modified couplings of Higgs with gauge bosons and fermions. For example, SUSY particles may alter the loop contribution in ggF channel [33]. Consequently signal in the invisible decay channel will be a combined effect due to the modified Higgs production cross section and its branching ratio in the invisible channel. Hence this makes it difficult to constrain only the invisible decay branching ratio of the Higgs $BR(H \to inv)$. Instead what can be constrained is in fact

$$R_{inv} \equiv \sigma_H^{BSM} BR(H \to inv)/\sigma_H^{SM} \tag{1}$$

where σ_H^{BSM} and σ_H^{SM} stand for the Higgs production cross sections in the framework of corresponding BSM and SM respectively. At leading order, the Higgs produced through ggF and decaying invisibly would be hard to detect because of soft missing transverse momentum ($\not{p}_T$). However, at higher orders in QCD for ggF, the Higgs can be produced in association with a single jet and one can then look for a considerably large missing transverse momentum along with a jet. Interestingly, such final states with a mono-jet have been analyzed with 1 fb^{-1} of data at $\sqrt{s} = 7$ TeV for both CMS [34] and ATLAS [35]. Using those results, R_{inv} 1 can be constrained and is found to be more than 10 at 95% CL with 1fb^{-1} data [36]. Moreover, the mono-jet search has also been analyzed by including a second hard jet [34] thus also including events from VBF and VH processes in the signal. It has been argued recently that at 4.7 fb^{-1} data at $\sqrt{s} = 7$ TeV, this can be reduced to $R_{inv} < 2$ and for 15 fb^{-1} of data at 8 TeV this can be further reduced to $R_{inv} < 0.9$[37]. One should note here that

even though the production cross-section is large the mono-jet searches are plagued by large V+jets ($V = W, Z$) background.

The most promising channel for the detection of an invisibly decaying Higgs is VBF since it has a relatively large cross section and has an unique event topology that can be used to effectively remove backgrounds [20, 23, 38]. The signal consists of jets moving in opposite directions with large rapidity gaps. A recent study has shown that R_{inv} as low as 0.21 can be probed with 30 fb^{-1} data at $\sqrt{s} = 14$ TeV and for $\sqrt{s} = 7$ TeV with 20 fb^{-1} it can be probed to as low as 0.4 with 95% CL [39]. We also revisit this analysis for 8 TeV an 14 TeV energies. The main drawback of VBF channels is that it has large systematic uncertainties and it is difficult to estimate the QCD background [38, 23].

The $t\bar{t}H$ channel has been studied in detail [40] for $\sqrt{s} = 14$ TeV LHC in both the semileptonic, $t\bar{t} \to WbWb \to l\nu bq\bar{q}b$, and as well as in the hadronic mode $\to q\bar{q}bq\bar{q}b$. The complex final state and the combinatorial background requires a very sophisticated analysis.

The cleanest channel by far is the associated production channel $VH(V = W, Z)$. Incidentally, the couplings between gauge boson and Higgs are not expected to deviate from the SM significantly because of the unitarity of the theory and restrictions from electroweak precision tests. As a consequence, in any BSM model, the parton level cross sections for VBF and ZH channels turn out to be very close to SM values. These channels therefore give a direct probe of the invisible branching ratios, unlike ggF. However, the WH channel is diluted by the inclusive W background which makes it difficult to use for detecting an invisible Higgs decay [41] where as the ZH channel is more promising because of the presence of two leptons from the Z boson decay. We study here the efficacy of this channel in detecting invisible branching ratio at $\sqrt{s} = 8$ TeV and $\sqrt{s} = 14$ TeV energies. Like earlier studies of this channel [21, 39, 41] we use the leptonic decay to identify the Z boson. In addition, we consider the hadronic decay mode, specifically decay to b quarks and investigate the viability of use of jet substructure and clustering methods for detection of b jets in reducing backgrounds.

3 Invisible Higgs signal via VBF

In this section we study the feasibility of finding the invisible Higgs signal through the VBF process which is the sub dominant process for the Higgs production in hadron colliders. This channel has been studied previously for 14 TeV LHC [20, 23, 37, 41] and very recently for 7 TeV and 8 TeV [39]. We also revisit this analysis for 8 TeV and 14 TeV LHC energy for the Higgs mass of 125 GeV using a different set of selection cut values. In this channel, the Higgs is produced through vector boson

fusion, where vector bosons originate by radiating off two initial quarks along with two jets,

$$\mathbf{pp \rightarrow qqh \rightarrow 2jets} + \not{\mathbf{p}}_{\mathbf{T}}. \tag{2}$$

The final state consists of two jets in the forward and backward directions with a wide separation in rapidity and a reasonably large $\not{p}_T$ due to the presence of non-interacting particles from Higgs decay. In addition to this pure VBF processes, there are some non VBF processes which also provide the same final state consisting of 2 jets and $\not{p}_T$. For instance, higher order QCD effects in ggF process can give rise to two jets in the final states because of a hard emission of partons from the initial states with a a non negligible cross section. The dominant SM background processes for this signal are due to $(W \rightarrow \ell\nu)$+jets, $(Z \rightarrow \nu\bar{\nu})$+jets, $t\bar{t}$ (tbW) and QCD. For W+jets, a significant background can arise if the lepton is not detected. Note that the background cross sections mimicking the signal are significantly large, and hence a sizable reduction is required to achieve a reasonable signal sensitivity. The signal and background processes are simulated using `MadGraph/Madevent` [42] and subsequently passed through `PYTHIA6` [43] for parton showering. In this study for all numerical calculations we use CTEQ6L [44] for parton distribution functions. In the process of showering, we adopt MLM matching[45] using default values set by the `MadGraph/MadEvent` suite to avoid double counting of jets. Jets are reconstructed using `FastJet` [46] with anti-$\mathrm{K_T}$ [47] algorithm using size parameter $R = 0.5$ and applying a jet p_T threshold of 40 GeV and $|\eta| < 4.5$. Notice that the signal is completely free from leptonic activities whereas background channels may contain leptons in the final state. Therefore, a leptonic veto might help to eliminate certain fraction of backgrounds. Leptons are selected with p_T^ℓ >10 GeV, $|\eta_\ell|$ <2.5. We compute missing transverse energy from the momenta of all visible particles. The following set of cuts are used in the simulation :

1. VBF selections: The leading jets in Higgs production through the VBF process is produced in the forward and backward direction and hence is expected to have a large rapidity gap. Therefore, we select events where the absolute rapidity difference between the two leading jets is $|\eta_{j1} - \eta_{j2}| = |\Delta\eta|$ >4. To ensure that the two jets are in the opposite direction, the product of rapidity of two jets are required to be, $\eta_{j1} \times \eta_{j2}$ <0.

2. Central Jet veto: For a pure VBF process, no jets with $p_T > 40$ GeV are expected in the central region, therefore we discard events if there be any jets in central region.

3. Lepton veto(LV): Since the signal has a pure hadronic topology, events with any lepton are vetoed out.

4. Selection of $\not{p}_T$: Events are required to have at least $\not{p}_T$ >100 (170) GeV for 8 (14) TeV energy.

Process	8 TeV		14 TeV	
	Production CS[pb]	After cuts CS[fb]	Production CS[pb]	After cuts CS[fb]
W+2jets(VBF)	76.5	4.5	167.9	6.3
W+2jets	18700	5.8	45900	18.7
W+3jets	10260	< 1	21000	13
Z+2jets(VBF)	19	6	43.2	6.7
Z+2jets	6000	16.5	14000	11.2
Z+3jets	2772	8.3	7300	17.8
tbW	140	< 1	< 1	< 1
Total Background		41.1		74
hjj(VBF)	1.73	7.3	4.3	8.7
hjj	6.7	1.2	24.5	1.3
Signal		8.5		10

Table 1: Event yields of the signal and backgrounds for the final state with two jets and $\not{p}_T$ via VBF channel for 8 TeV and 14 TeV LHC energies. In the second column the cross sections corresponding to production and after all cuts are shown for signal and background processes respectively for 8 TeV energy. The third column presents the same for 14 TeV energy.

5. Dijet invariant mass M_{jj} : The invariant mass of two leading jets is expected to be very large and hence we demand, M_{jj} >1400 (1800) GeV for 8 TeV (14 TeV) energy.

We notice that $\not{p}_T$ and M_{jj} cuts are very useful to suppress the backgrounds with a marginal effect in the signal cross section. We have also checked that the background contribution due to QCD is negligible because of a strong $\not{p}_T$ and a large di-jet invariant mass cut(M_{jj}); this is why results for QCD are not presented here. In Table 1 we present the event summary for signal and all background processes subjected to the above set of cuts. The first column represents the production cross section at the leading order obtained from `MadGraph` [42]. The contribution due to the pure VBF type and non-VBF type of processes are shown separately. In the subsequent columns, the cross sections subject to all cuts are presented. Notably, there exists a non negligible possibility that W/Z+3jet channel may contribute to the background cross section, if the third jet is not detected. Here we present our results for both the 8 TeV and 14 TeV energies. At 8 TeV energy, for $\mathcal{L}$=20fb^{-1}, it is possible to observe signal with S/$\sqrt{B}$ $\sim$5.9 leading to a detection of invisible BR $\sim$84% or above assuming $\sigma_{SM} = \sigma_{BSM}$ in Eq. 1. On the other hand, for 14 TeV energy, results are more encouraging

where one can find a signal with a better sensitivity yielding S/$\sqrt{B}$ $\sim$ 6.3 (20) for 30 (300) fb^{-1} integrated luminosity which predicts a measurement of BR $\geq$ 0.79(0.25). It is to be noted that in our calculation we used LO cross sections for both signal and backgrounds. However the K-factor for the signal is $\sim$0.95 [48] and for W/Z+jets it is also very close to 1($\sim$1.1) [49, 50]. Therefore, inclusion of K-factors in the above calculation will not alter the conclusions significantly.

4 Invisible Higgs signal via ZH

Here we study the signature of the invisible decay of Higgs via the ZH channel, where Z can decay both leptonically and hadronically, $Z \to \ell\bar{\ell}, b\bar{b}$. It is well known from an experimental point of view that the leptonic channel is comparatively cleaner than the hadronic channel consisting of b-jets. However we simulate both these channels to find the detectability of an invisible Higgs decay. In the following, we describe our simulation for both the final states.

(a) $\underline{Z \to \ell\bar{\ell}}$

Here the final states consist of two leptons with opposite charge and same flavor and with a considerable amount of missing transverse momentum due to the Higgs decay into invisible particles. This channel was studied extensively in an earlier study for 14 TeV LHC energy [21]. The main dominant SM backgrounds are expected from the following processes,

1. ZZ production with one Z decaying to neutrinos and the other Z decaying leptonically. Clearly, this background has exactly identical characteristics to the signal.

2. WZ production followed by the leptonic decays of both the W and Z, giving rise to $\ell\nu_\ell\bar{\ell}\ell$ where one of the leptons is lost.

3. WW production with both W bosons decaying leptonically, $W \to \ell\nu_\ell$.

4. Top pair production, $t\bar{t} \to WWb\bar{b} \to l\nu_l\bar{l}\bar{\nu_l}b\bar{b}$ which may appear signal-like if the b-jets escape detection.

The Higgs being heavier in comparison to the particles in the background processes other than the top quark, gives rise to a harder $\not{p}_T$. Therefore, demanding a large $\not{p}_T$ one can efficiently reduce backgrounds. In the signal topology, an added advantage is that the invariant mass of two leptons peaks around the mass of the Z boson. Hence requiring the di-lepton invariant mass to be around the mass of the Z boson, it is possible to suppress backgrounds partially except for the ZZ process.

Since the Z boson and the Higgs are more likely produced back to back, the transverse mass of the di-lepton system and the $\not{p}_T$, defined as,

$$M_T^{l\bar{l}} = \sqrt{p_T^{ll} \not{p}_T \left(1 - cos\phi(E_T^{ll}, \not{p}_T)\right)}, \tag{3}$$

has a softer distribution for all background processes. Therefore, demanding a large value for this variable enables us to eliminate backgrounds substantially.

As before, we use `MadGraph`[42] to generate both the signal and background processes which are subsequently passed through `PYTHIA6` [43] for event generation including showering. We apply the following set of cuts in our simulation for the event selection and as well as suppressing the background events.

1. Select leptons with $p_T^\ell > 10$ GeV and $|\eta_l| < 3$. The isolation of lepton is ensured by looking at the total transverse energy $E_T^{ac} \leq 20\%$ of the p_T of lepton, where E_T^{ac} is the scalar sum of the transverse energies of jets within a cone of size $\Delta R(l, j) \leq 0.2$ between the jet and the lepton.
2. Since final states are hadronically quiet, vetoing events consisting jets, with $p_T > 30$ GeV and $|\eta| < 4$ are useful in eliminating certain fraction of backgrounds.
3. Azimuthal angle between two leptons, $\cos\phi_{\ell\bar{\ell}} > 0$ and transverse mass between two leptons and $\not{p}_T$, $M_T^{l\bar{l}} > 150$ (200) GeV for 8 (14) TeV energies.
4. Missing transverse momentum, $\not{p}_T$ >100 GeV.
5. Di-lepton invariant mass, $|M_Z - m_{\ell\bar{\ell}}| < 10$ GeV.

For 14 TeV LHC energy, the strategy of simulation is not significantly different as no additional effects occur. The same set of cuts with similar thresholds are used with the only exception of $M_T^{\ell\bar{\ell}}$ where 200 GeV is used instead of 150 GeV. In Table 2, we display event yields for both signal and backgrounds for 8 and 14 TeV energies. In each column, numbers in left side stand for the production cross sections corresponding to energies as shown in the respective columns. For both energies, we find that $M_T^{l\bar{l}}$ and $\not{p}_T$ play a very useful role in suppressing the backgrounds. The kinematics of ZZ process is identical to that of the signal process although there is a moderate mass difference (35 GeV) between the Z and the Higgs boson, resulting in a similar effect of cuts on both signal and ZZ background. As a consequence, ZZ turns out to be the dominant irreducible background. The numbers in the right hand side of each column show the final cross sections after being multiplied by acceptance efficiencies. For 8 TeV energy with an integrated luminosity of $\mathcal{L}$=20 fb^{-1} we find

Process	8 TeV		14 TeV	
	Production C.S[pb]	After Cuts C.S[fb]	Production C.S[pb]	After Cuts C.S[fb]
ZZ	4.79	6.7	10.1	17.6
WZ	12.6	1.8	47.3	3.8
WW	33.8	0.3	69.4	2.3
$t\bar{t}$	115	0.1	480	0.95
Total Bg		8.9		24.7
ZH	0.3	2.3	0.64	5.6

Table 2: Event yields for the dilepton+$\not{p}_T$ final states. In the second and third columns, the production cross sections and cross sections after selection cuts, as described in the text, are presented for 8 TeV and 14 TeV center of mass energies respectively.

S/$\sqrt{B}$ $\sim$ 3.5 i.e., the signal is observable. However, for 14 TeV energy with $\mathcal{L}$=50 fb^{-1} one can observe the invisible signal with signal significance of $\sim$8. Note that the estimations are based on LO cross sections. However, we note that the K-factors for vector boson production and for the signal process are 1.6-1.7 [51] and 1.3[32] respectively. Hence we do not expect any major changes in our results.

(b)<u>Z $\rightarrow b\bar{b}$</u>

In this section we explore the possibility of detecting invisible Higgs decay channel by identifying two b-jets arising from Z boson decay. We analyze this channel following two methods. In the first method, b-jets are identified by using the standard jet clustering algorithm and in the second method, jet substructure technique[25] is used. However, in both cases the dominant SM backgrounds arise from:

1. irreducible background from ZZ production with one Z decaying to neutrinos and the other Z decaying to b quarks.
2. QCD background with Z produced in association with two b quarks and the Z boson decaying to neutrinos, ($Zb\bar{b} \rightarrow \nu\bar{\nu}b\bar{b}$).
3. WZ production with the W decaying leptonically, and the Z decaying to b-quarks and the lepton is lost, ($WZ \rightarrow l\nu_l b\bar{b}$)
4. $t\bar{t}$ production where two b-jet from top decays are identified and rest of the event objects are

lost.

5. W boson produced in association with b quarks ($Wb\bar{b}$) where W decays leptonically and the lepton is not identified.

The event topology of this channel is not significantly different to the di-lepton final stats as discussed above, and hence we apply similar type of cuts. Absence of any detectable hard lepton in the final state leads us to apply a lepton veto to reduce backgrounds, in particular from $t\bar{t}$, WZ and $Wb\bar{b}$ production. As before, $M_T^{b\bar{b}}$, the transverse mass between two b-jets and $\not{p}_T$ distributions of the backgrounds are soft. Therefore, selection of signal events corresponding to large values of these kinematic variables helps to remove significant fraction of the backgrounds. Moreover, we construct another useful variable, R_T, to remove large amount of the QCD. [52, 53, 54, 55, 56]. This variable is defined as,

$$R_T = \frac{p_{T_{b_{j_1}}} + p_{T_{b_{j_2}}}}{H_T}, \tag{4}$$

where H_T is the scalar sum of the transverse momenta of all detected jets including all non-tagged jets. Since one expects less non-tagged jet activity in signal,R_T would tend to have larger values ($\sim$ 1) as compared to the events arising from QCD and other backgrounds. Naturally, requiring R_T to have a large value($\sim$ 1), leads to a substantial suppression of backgrounds, particularly for those due to QCD processes.

We simulate as before the signal and backgrounds using `MadGraph` [42] applying the following set of selection cuts:

1. Select b-jets by performing a matching between b quarks and jets using matching cone $\Delta R = 0.3$ and finally multiply a b-tagging efficiency of 0.6 [57] for each of the b-jets. In the jet substructure method we employ mass drop techniques described in [25] to find the subjets which are also identified as a b-like jets by flavor matching.

2. Veto events with leptons, where $p_T^l > 10$ GeV and $|\eta_l| < 3$.

3. Select dijet events with both jets b-like and ensure that $|M_{b\bar{b}} - M_Z| < 30$ GeV.

4. $\not{p}_T > 70$ GeV.

5. $M_T(b\bar{b}, \not{p}_T)$ >200 GeV.

6. $R_T > 0.9$.

Process	Production C.S[pb]	After Cuts C.S [fb] b jet cluster	After cuts C.S[fb] b jet substructure
ZZ	4.79	2.26	1.92
WZ	12.6	0.38	0.36
$\nu\bar{\nu}b\bar{b}$	16	3.1	1.33
$t\bar{t}$	115	0.48	0.52
W$b\bar{b}$	50.5	0.54	0.16
Background		6.76	4.29
ZH	0.3	0.8	0.72

Table 3: Event yields for the final states with b jet pairs and $\not{p}_T$ for 8 TeV energy. The last two columns show the final cross sections after all cuts as described in the text.

In Table 3 we present the final results of the simulation for both methods for 8 TeV energy. The second column presents the total production cross sections corresponding to each processes and subsequent columns show cross section after applying above set of cuts. However, in both cases, for an integrated luminosity of $\mathcal{L}$ = 20 fb^{-1} the best we can achieve is S/$\sqrt{B}$ $\sim$ 2. In Table 4 as before, we present results for 14 TeV LHC energy. Here also we find that we can achieve a modest S/$\sqrt{B}$ $\sim$ 4 with an integrated luminosity of $\mathcal{L}$=100 fb^{-1}. However, for a very high luminosity option, e.g $\mathcal{L}$=300 fb^{-1}, for a moderate value of signal events, one can expect to observe an invisible BR of Higgs $\sim$75% or more. Note that because of low b-jet acceptance efficiency and irreducible ZZ backgrounds this final state yield a marginal sentivity. As we see jet substructure method does not give substantially better

Process	Production C.S[pb]	After Cuts C.S [fb] b jet cluster	After cuts C.S[fb] b jet substructure
ZZ	10	5.56	2.47
WZ	26.7	3.5	1.44
$\nu\bar{\nu}b\bar{b}$	47.3	12.9	3.04
$t\bar{t}$	476	3.92	0.16
W$b\bar{b}$	112	4.2	1.08
Background		30.	8.19
ZH	0.64	2.	1.1

Table 4: Same as Table 3, but for 14 TeV LHC energy.

results because of the fact that the Z boson is not sufficiently boosted. Like the dilepton scenario

as explained before, our results do not change significantly with the inclusion of higher order cross sections by using appropriate K factors.

5 Summary

Recent discovery of a Higgs like resonance by both the experimental groups: CMS and ATLAS has now spurred a series of investigations to determine whether it is 'a' Higgs boson and if so it is 'the SM' Higgs boson. Assuming that it is 'a' Higgs boson the current experimental information still does not rule out the possibility of BSM physics. Many BSM models predict decay of the Higgs in the invisible channel along with the usual SM decay modes. Such invisible decay modes, if confirmed or ruled out, will allow us to indirectly probe BSM physics. In this note we revisit the possibility of looking for a Higgs boson decaying invisibly, for two production channels for the Higgs : the vector boson fusion channel (VBF) as well as the associated production of Higgs with Z (ZH), for two different LHC energies: 8 and 14 TeV. In the ZH case, we also investigate the possibility of using the $Z \to b\bar{b}$ channel. We note that in the VBF channel the sensitivity is more than 5σ at both the energies : 8 and 14 TeV for large invisible branching ratios (> 0.8) for integrated luminosity of 20 fb^{-1} and 30 fb^{-1}, whereas at 14 TeV with 300 fb^{-1} one can reach an invisible branching ratio as low as 0.25. In the ZH channel with dileptonic decay of the Z, the sensitivity with the planned luminosity of 20 fb^{-1} is limited at 8 TeV and rises to 8σ at 14 TeV with 50 fb^{-1}. With the $b\bar{b}$ final state, with 20fb^{-1} we can only reach $S/\sqrt{B} \sim 2$ at 8 TeV energy, where as with high luminosity (~ 300 fb^{-1}) and at 14 TeV energy we can probe the invisible decay at 5σ level, for an invisible branching ratio above 0.75. As we find the determination of an invisible branching fraction at the LHC is comparatively difficult, an electron-positron collider the associated production of the Higgs with a Z boson provides an extremely clean channel to study invisible branching ratio [58, 59].

6 Acknowledgements

DG acknowledges support from ERC Ideas Starting Grant n. 279972 "NPFlavour". DG also acknowledges the hospitality at the Centre for High Energy Physics, IISc where part of this work was completed. RMG wishes to acknowledge the Department of Science and Technology of India, for financial support under the J.C. Bose Fellowship scheme under grant no. SR/S2/JCB-64/2007. MG acknowledges John Alwall for help regarding matching in the context of MadEvent and V. Ravindran

for useful discussion related with Higgs cross sections. KM acknowledges CSIR fellowship. KM also acknowledges the Department of High Energy Physics, Tata Institute of Fundamental Research for the hospitality where part of the work was done.

References

[1] S. Glashow, "Partial Symmetries of Weak Interactions," *Nucl.Phys.* **22** (1961) 579–588.

[2] S. Weinberg, "A Model of Leptons," *Phys.Rev.Lett.* **19** (1967) 1264–1266.

[3] A. Salam, "Weak and Electromagnetic Interactions," *Conf.Proc.* **C680519** (1968) 367–377.

[4] **ATLAS** Collaboration, G. Aad *et al.*, "Observation of a new particle in the search for the Standard Model Higgs boson with the ATLAS detector at the LHC," *Phys.Lett.* **B716** (2012) 1–29, `arXiv:1207.7214 [hep-ex]`.

[5] **CMS** Collaboration, S. Chatrchyan *et al.*, "Observation of a new boson at a mass of 125 GeV with the CMS experiment at the LHC," *Phys.Lett.* **B716** (2012) 30–61, `arXiv:1207.7235 [hep-ex]`.

[6] G. Bertone, D. Hooper, and J. Silk, "Particle dark matter: Evidence, candidates and constraints," *Phys.Rept.* **405** (2005) 279–390, `arXiv:hep-ph/0404175 [hep-ph]`.

[7] G. Altarelli and F. Feruglio, "Models of neutrino masses and mixings," *New J.Phys.* **6** (2004) 106, `arXiv:hep-ph/0405048 [hep-ph]`.

[8] A. Denner, S. Heinemeyer, I. Puljak, D. Rebuzzi, and M. Spira, "Standard Model Higgs-Boson Branching Ratios with Uncertainties," *Eur.Phys.J.* **C71** (2011) 1753, `arXiv:1107.5909 [hep-ph]`.

[9] G. Belanger, F. Boudjema, A. Cottrant, R. Godbole, and A. Semenov, "The MSSM invisible Higgs in the light of dark matter and g-2," *Phys.Lett.* **B519** (2001) 93–102, `arXiv:hep-ph/0106275 [hep-ph]`.

[10] G. F. Giudice, R. Rattazzi, and J. D. Wells, "Graviscalars from higher dimensional metrics and curvature Higgs mixing," *Nucl.Phys.* **B595** (2001) 250–276, `arXiv:hep-ph/0002178 [hep-ph]`.

[11] M. Battaglia, D. Dominici, J. Gunion, and J. Wells, "The Invisible Higgs decay width in the add model at the LHC," `arXiv:hep-ph/0402062 [hep-ph]`.

[12] S. Gopalakrishna, S. J. Lee, and J. D. Wells, "Dark matter and Higgs boson collider implications of fermions in an abelian-gauged hidden sector," *Phys.Lett.* **B680** (2009) 88–93, `arXiv:0904.2007 [hep-ph]`.

[13] K. Ghosh, B. Mukhopadhyaya, and U. Sarkar, "Signals of an invisibly decaying Higgs in a scalar dark matter scenario: a study for the Large Hadron Collider," *Phys.Rev.* **D84** (2011) 015017, `arXiv:1105.5837 [hep-ph]`.

[14] J. R. Espinosa, M. Muhlleitner, C. Grojean, and M. Trott, "Probing for Invisible Higgs Decays with Global Fits," `arXiv:1205.6790 [hep-ph]`.

[15] D. Carmi, A. Falkowski, E. Kuflik, T. Volansky, and J. Zupan, "Higgs After the Discovery: A Status Report," `arXiv:1207.1718 [hep-ph]`.

[16] P. P. Giardino, K. Kannike, M. Raidal, and A. Strumia, "Is the resonance at 125 GeV the Higgs boson?," `arXiv:1207.1347 [hep-ph]`.

[17] **LEP Higgs Working for Higgs boson searches, ALEPH Collaboration, DELPHI Collaboration, CERN-L3 Collaboration, OPAL Collaboration** Collaboration, "Searches for invisible Higgs bosons: Preliminary combined results using LEP data collected at energies up to 209-GeV," `arXiv:hep-ex/0107032 [hep-ex]`.

[18] J. Gunion, "Detecting an invisibly decaying Higgs boson at a hadron supercollider," *Phys.Rev.Lett.* **72** (1994) 199–202, `arXiv:hep-ph/9309216 [hep-ph]`.

[19] D. Choudhury and D. Roy, "Signatures of an invisibly decaying Higgs particle at LHC," *Phys.Lett.* **B322** (1994) 368–373, `arXiv:hep-ph/9312347 [hep-ph]`.

[20] O. J. Eboli and D. Zeppenfeld, "Observing an invisible Higgs boson," *Phys.Lett.* **B495** (2000) 147–154, `arXiv:hep-ph/0009158 [hep-ph]`.

[21] R. Godbole, M. Guchait, K. Mazumdar, S. Moretti, and D. Roy, "Search for 'invisible' Higgs signals at LHC via associated production with gauge bosons," *Phys.Lett.* **B571** (2003) 184–192, `arXiv:hep-ph/0304137 [hep-ph]`.

[22] V. Barger, M. Ishida, and W.-Y. Keung, "Total Width of 125 GeV Higgs Boson," *Phys.Rev.Lett.* **108** (2012) 261801, `arXiv:1203.3456 [hep-ph]`.

[23] B. Di Girolamo, A. Nikitenko, L. Neukermans, K. Mazumdar, and D. Zeppenfeld, "Experimental observation of an invisible Higgs boson at LHC," tech. rep., 2001.

[24] H. Davoudiasl, T. Han, and H. E. Logan, "Discovering an invisibly decaying Higgs at hadron colliders," *Phys.Rev.* **D71** (2005) 115007, `arXiv:hep-ph/0412269 [hep-ph]`.

[25] J. M. Butterworth, A. R. Davison, M. Rubin, and G. P. Salam, "Jet substructure as a new Higgs search channel at the LHC," *Phys.Rev.Lett.* **100** (2008) 242001, `arXiv:0802.2470 [hep-ph]`.

[26] **LHC Higgs Cross Section Working Group** Collaboration, S. Dittmaier *et al.*, "Handbook of LHC Higgs Cross Sections: 1. Inclusive Observables," `arXiv:1101.0593 [hep-ph]`.

[27] S. Dawson, "Radiative corrections to Higgs boson production," *Nucl.Phys.* **B359** (1991) 283–300.

[28] A. Djouadi, M. Spira, and P. Zerwas, "Production of Higgs bosons in proton colliders: QCD corrections," *Phys.Lett.* **B264** (1991) 440–446.

[29] R. V. Harlander and W. B. Kilgore, "Next-to-next-to-leading order Higgs production at hadron colliders," *Phys.Rev.Lett.* **88** (2002) 201801, `arXiv:hep-ph/0201206 [hep-ph]`.

[30] C. Anastasiou and K. Melnikov, "Higgs boson production at hadron colliders in NNLO QCD," *Nucl.Phys.* **B646** (2002) 220–256, `arXiv:hep-ph/0207004 [hep-ph]`.

[31] V. Ravindran, J. Smith, and W. L. van Neerven, "NNLO corrections to the total cross-section for Higgs boson production in hadron hadron collisions," *Nucl.Phys.* **B665** (2003) 325–366, `arXiv:hep-ph/0302135 [hep-ph]`.

[32] J. Baglio and A. Djouadi, "Higgs production at the lHC," *JHEP* **1103** (2011) 055, `arXiv:1012.0530 [hep-ph]`.

[33] A. Djouadi, "The Anatomy of electro-weak symmetry breaking. I: The Higgs boson in the standard model," *Phys.Rept.* **457** (2008) 1–216, `arXiv:hep-ph/0503172 [hep-ph]`.

[34] **CMS** Collaboration, "Search for new physics with a monojet and missing transverse energy in pp collisions at sqrt(s) = 7 tev," Tech. Rep. CMS-PAS-EXO-11-059, CERN, Geneva, 2011. `http://cdsweb.cern.ch/record/1376675`.

[35] **ATLAS** Collaboration, G. Aad *et al.*, "Search for new phenomena with the monojet and missing transverse momentum signature using the ATLAS detector in $\sqrt{s} = 7$ TeV proton-proton collisions," *Phys.Lett.* **B705** (2011) 294–312, `arXiv:1106.5327 [hep-ex]`.

[36] C. Englert, J. Jaeckel, E. Re, and M. Spannowsky, "Evasive Higgs Maneuvers at the LHC," *Phys.Rev.* **D85** (2012) 035008, `arXiv:1111.1719 [hep-ph]`.

[37] A. Djouadi, A. Falkowski, Y. Mambrini, and J. Quevillon, "Direct detection of Higgs-portal dark matter at the LHC," `arXiv:1205.3169 [hep-ph]`.

[38] S. Bansal, K. Mazumdar, and J. Singh, "Search for invisibly decaying Higgs boson at Large Hadron Collider," *Pramana* **74** (2010) 231–246.

[39] Y. Bai, P. Draper, and J. Shelton, "Measuring the Invisible Higgs Width at the 7 TeV LHC," *JHEP* **1207** (2012) 192, `arXiv:1112.4496 [hep-ph]`.

[40] B. P. Kersevan, M. Malawski, and E. Richter-Was, "Prospects for observing an invisibly decaying Higgs boson in the t anti-t H production at the LHC," *Eur.Phys.J.* **C29** (2003) 541–548, `arXiv:hep-ph/0207014 [hep-ph]`.

[41] **ATLAS** Collaboration, P. Gagnon *et al.*, "Sensitivity to an invisibly decaying Higgs boson," Tech. Rep. ATL-PHYS-PUB-2009-061, ATL-COM-PHYS-2009-220, 2009.

[42] J. Alwall, M. Herquet, F. Maltoni, O. Mattelaer, and T. Stelzer, "MadGraph 5 : Going Beyond," *JHEP* **1106** (2011) 128, `arXiv:1106.0522 [hep-ph]`.

[43] T. Sjostrand, S. Mrenna, and P. Z. Skands, "PYTHIA 6.4 Physics and Manual," *JHEP* **0605** (2006) 026, `arXiv:hep-ph/0603175 [hep-ph]`.

[44] J. Pumplin, D. Stump, J. Huston, H. Lai, P. M. Nadolsky, *et al.*, "New generation of parton distributions with uncertainties from global QCD analysis," *JHEP* **0207** (2002) 012, `arXiv:hep-ph/0201195 [hep-ph]`.

[45] S. Hoeche, F. Krauss, N. Lavesson, L. Lonnblad, M. Mangano, *et al.*, "Matching parton showers and matrix elements," `arXiv:hep-ph/0602031 [hep-ph]`.

[46] M. Cacciari, G. P. Salam, and G. Soyez, "FastJet User Manual," *Eur.Phys.J.* **C72** (2012) 1896, `arXiv:1111.6097 [hep-ph]`.

[47] M. Cacciari, G. P. Salam, and G. Soyez, "The Anti-k(t) jet clustering algorithm," *JHEP* **0804** (2008) 063, `arXiv:0802.1189 [hep-ph]`.

[48] T. Figy, S. Palmer, and G. Weiglein, "Higgs Production via Weak Boson Fusion in the Standard Model and the MSSM," *JHEP* **1202** (2012) 105, `arXiv:1012.4789 [hep-ph]`.

[49] C. Berger, Z. Bern, L. J. Dixon, F. Febres Cordero, D. Forde, *et al.*, "Precise Predictions for W + 4 Jet Production at the Large Hadron Collider," *Phys.Rev.Lett.* **106** (2011) 092001, `arXiv:1009.2338 [hep-ph]`.

[50] H. Ita, Z. Bern, L. Dixon, F. Febres Cordero, D. Kosower, *et al.*, "Precise Predictions for Z + 4 Jets at Hadron Colliders," *Phys.Rev.* **D85** (2012) 031501, arXiv:1108.2229 [hep-ph].

[51] J. M. Campbell, R. K. Ellis, and C. Williams, "Vector boson pair production at the LHC," *JHEP* **1107** (2011) 018, arXiv:1105.0020 [hep-ph].

[52] M. Guchait and D. Sengupta, "Event-shape selection cuts for supersymmetry searches at the LHC with 7 TeV energy," *Phys.Rev.* **D84** (2011) 055010, arXiv:1102.4785 [hep-ph].

[53] R. M. Chatterjee, M. Guchait, and D. Sengupta, "Probing Supersymmetry using Event Shape variables at 8 TeV LHC," *Phys.Rev.* **D86** (2012) 075014, arXiv:1206.5770 [hep-ph].

[54] D. Ghosh, M. Guchait, S. Raychaudhuri, and D. Sengupta, "How Constrained is the cMSSM?," *Phys.Rev.* **D86** (2012) 055007, arXiv:1205.2283 [hep-ph].

[55] D. Ghosh, M. Guchait, and D. Sengupta, "Higgs Signal in Chargino-Neutralino Production at the LHC," *Eur.Phys.J.* **C72** (2012) 2141, arXiv:1202.4937 [hep-ph].

[56] P. Byakti and D. Ghosh, "Magic Messengers in Gauge Mediation and signal for 125 GeV boosted Higgs boson," *Phys.Rev.* **D86** (2012) 095027, arXiv:1204.0415 [hep-ph].

[57] **CMS** Collaboration, "Performance of the b-jet identification in CMS," Tech. Rep. CMS-PAS-BTV-11-001, 2011.

[58] M. Schumacher, "Investigation of invisible decays of the Higgs boson at a future e+ e- linear collider," Tech. Rep. LC-PHSM-2003-096, 2003.

[59] F. Richard and P. Bambade, "Strategy to measure the Higgs mass, width and invisible decays at ILC," arXiv:hep-ph/0703173 [HEP-PH].